Journal of Molecular Graphics and Modelling 28 (2010) 548–554

Contents lists available at ScienceDirect

Journal of Molecular Graphics and Modelling

journal homepage: www.elsevier.com/locate/JMGM

Mechanical unfolding of bacterial flagellar filament protein by molecular dynamics simulation

Choon-Peng Chng [a,1], Akio Kitao [b,c,*]

[a] Department of Computational Biology, Graduate School of Frontier Sciences, University of Tokyo, Japan
[b] Laboratory of Molecular Design, Institute of Molecular and Cellular Biosciences, University of Tokyo, 1-1-1 Yayoi, Bunkyo-ku, Tokyo 113-0032, Japan
[c] Japan Science and Technology Agency, Core Research for Evolutional Science and Technology, Tokyo, Japan

ARTICLE INFO

Article history:
Received 20 August 2009
Accepted 30 November 2009
Available online 4 December 2009

Keywords:
Flagellin
Flagellar export
Force-denaturation
Protein mechanics
Multi-domain

ABSTRACT

Bacterial flagellum is a nano-scale motility device constructed by self-assembly. During construction of the cell-exterior filament (the 'propeller'), subunit proteins (called flagellin) are thought to be exported through the hollow flagellum to the growing filament tip in an unfolded state. To gain insight into the unfolded state preceding any force-spectroscopy experiments on flagellin, we employed force-probe molecular dynamics simulations. Two schemes to attain an unfolded state suitable for efficient transport were examined: (i) stretching flagellin along its length; (ii) unzipping flagellin from its adjacently placed termini. Atomic-level unfolding pathways and the mechanical efforts involved under each scheme were obtained for the four-domain flagellin from *S. typhimurium*. Flagellin appeared stiffer and required larger unfolding forces when stretched as the relative sliding of β-strands require the breaking of multiple hydrogen bonds at once. In contrast, unzipping requires lower unfolding forces as it mainly involves unraveling β-sheets by breaking hydrogen bonds one by one.

1. Introduction

The bacterial flagellum is a protein-based motility device. It consists of a micrometer-long screw-like tubular filament driven by a membrane-embedded rotary motor that is powered by a flow of protons or sodium ions. During self-assembly of the flagellum, proteins destined for the cell-exterior components have to be exported by the flagellar export apparatus after synthesis [1]. For filament construction, each of the subunit proteins known as flagellin has to be transported through a continuous channel to reach the site of assembly at the filament tip, where a capping protein complex assists in flagellin polymerization and prevents flagellin loss [2].

The flagellar channel diameter of 20 Å may be too narrow for a folded multi-domain flagellin to pass through: the complete 3D structure for *Salmonella typhimurium* flagellin obtained at atomic resolution [3] shows the presence of β-sheet rich domains which have cross-sections larger than 20 Å (Fig. 1). These so-called Hypervariable Region (HVR) domains are encoded by a stretch of amino-acid sequence in the middle of the flagellin sequence that varies greatly in composition and length among homologues [4]. It is likely for other homologues that contain HVR of similar length to encode similarly large domains. If the inner diameter of the filament could somehow expand in response to moving molecules, it would be possible to transport flagellin molecules in a largely folded state. However, to our knowledge there is no experimental evidence to support this possibility. Furthermore, hydrophobic interactions mediating coiled-coil formation between terminal helices of adjacent polymerized flagellin contributing to mechanical stability of the filament [3] might also limit how much the channel diameter can expand. MD simulations of a 44-flagellin segment of the filament showed relatively small fluctuations in the central channel diameter on the nanosecond time-scale [5]. Hence it is more likely for flagellin (and possibly other flagellar export proteins) to be transported in a partially if not completely unfolded form, as suggested by Namba and co-workers [3].

For flagellar proteins to be largely or completely unfolded during transport, they could have been either (i) maintained in an unfolded state after their synthesis or (ii) actively unfolded before transport. To date the only known chaperone of flagellin, FliS, binds to the partially structured C-terminal segment to inhibit cytoplasmic polymerization of flagellin while leaving the rest of the molecule folded [6,7]. Hence, flagellar proteins are likely to be largely folded in the cytoplasm while waiting to be exported. As proteins are unfolded mechanically for various processes such as membrane translocation or degradation [8], it is highly likely that

* Corresponding author at: Laboratory of Molecular Design, Institute of Molecular and Cellular Biosciences, University of Tokyo, 1-1-1 Yayoi, Bunkyo-ku, Tokyo 113-0032, Japan. Tel.: +81 3 5841 2297; fax: +81 3 5841 2297.
E-mail address: kitao@iam.u-tokyo.ac.jp (A. Kitao).
[1] Present address: Biophysics Team, A*STAR Institute of High Performance Computing, 1 Fusionopolis Way, #16-16 Connexis, Singapore 138632, Singapore.

1093-3263/$ – see front matter © 2009 Elsevier Inc. All rights reserved.
doi:10.1016/j.jmgm.2009.11.007

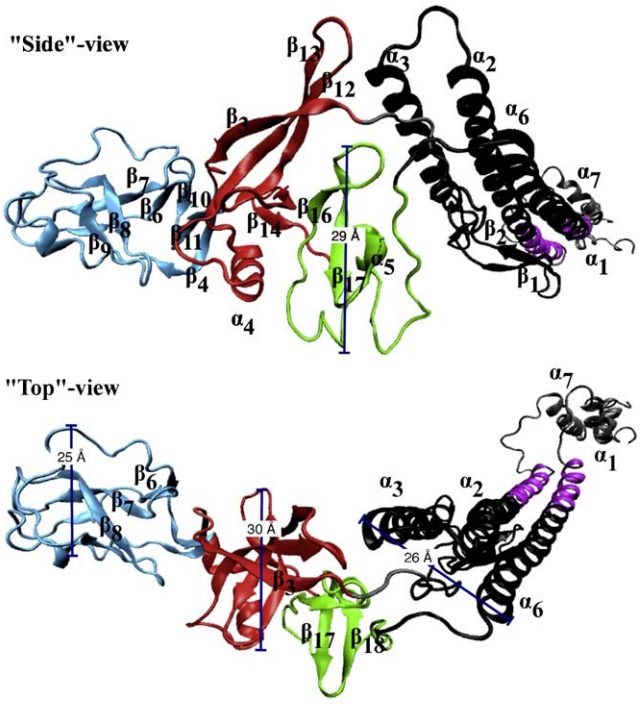

Fig. 1. Two views of the conformation of monomeric flagellin obtained from PDBid 1UCU by molecular dynamics simulation. Domains are colored as follows: D0 helices in gray, D1 in black and magenta, with proteolytic-resistant segment D_f1 in black, subdomain D2a in red and D2b in green, and D3 in light blue. Rough estimates of the cross-section of some domains are indicated.

the flagellar export apparatus also unfold flagellin mechanically though the origin of the force remains controversial [9].

For efficient transport and assembly, the multi-domain flagellin may have been evolutionarily designed to unfold easily under tension yet quick to refold from the denatured state. Using thermal unfolding simulations of flagellin, we have found suggestions that the (re)folding process might be accelerated with the formation of three-stranded Z-like β-sheets as folding nuclei in the β-rich HVR domains [10]. Would flagellin also unravel easily when pulled upon by the flagellar export system? As the mechanical response of protein molecules are known to be dependent on how they are deformed [11,12], could there be any preferred direction to unfold flagellin with minimal effort? For instance, Titin mutants showing less resistance to mechanical unfolding by Atomic Force Microscopy (AFM) are also more easily imported into mitochondria [13]. An understanding of the mechanical response of flagellin might thus provide insight into the export process. As no single-molecule force-spectroscopy experiments have been reported for flagellin, we wish to use computer simulations to gain some preliminary insights. Force-probe [14] or steered molecular dynamics (SMD) simulations [15] have shown some success at mimicking AFM action *in silico*. They also serve to complement AFM experiments by revealing the unfolding pathway in atomic detail [16,17].

In this study, we explored how to mechanically deform flagellin so as to attain a conformation suitable for transport through the narrow flagellar channel by means of force-probe MD simulations. Two conveniently chosen but also most extreme pulling schemes were investigated here. In the first scheme, termed *Unzip*, flagellin is unraveled from its adjacently placed termini into a linear polypeptide. In the second scheme, termed *Stretch*, flagellin is stretched along its major principal axis into a hairpin-like conformation (by virtue of its "fold-back" topology). We have quantified the associated mechanical efforts and identified the load-bearing elements encountered along the unfolding pathways in each scheme. These could help to interpret future single-molecule force-spectroscopy experiments on flagellin. We found that *Unzip* may be the more likely of the two schemes investigated here to produce a transport-capable flagellin.

2. Methods

2.1. Monomeric flagellin structures

We first explain the procedure to prepare equilibrated models of *monomeric* flagellin in explicit solvent before describing how starting structures for mechanical unfolding are generated.

The atomic coordinates of flagellin was taken from PDBid 1UCU [3], solved as a subunit of the bacterial filament of *Salmonella typhimurium* (*polymeric* flagellin). *S. typhimurium* flagellin has 494 residues contained in four domains, with terminal helical domains D0, D1 being highly conserved across bacterial species [4] as they form the inner and outer filament tubes responsible for filament structure integrity [3]. The remaining two outer domains (D2, D3) encoded by the mid portion of the amino-acid sequence are called Hypervariable Region (HVR) domains as they vary significantly in size and composition among homologues. D2 of *S. typhimurium* consists of subdomains D2a and D2b. We obtained the conformation of free (*monomeric*) flagellin in solution from the structure of *polymeric* flagellin. The procedure is outlined in our thermal unfolding study of flagellin [10]. The flagellin conformer after 1.4-ns of NPT production MD in explicit solvent was taken as the *monomeric* form of flagellin (Fig. 1) and denoted as *S1_pre*. For an alternative *monomeric* flagellin conformer, we used the 3.3-ns snapshot from the 8-ns NVE control simulation in our thermal unfolding study (denoted as *S2_pre*).

2.2. Force-probe simulations

Force-probe MD simulations initially were carried out in a very long explicit solvent box to accommodate the elongated flagellin molecule (~170 Å) but later found to be impractical. Implicit solvent models were then chosen for their much lower computation cost, despite the limitations (see Section 3). Specifically, the OBC model II variant [18] of the Generalized-Born/Surface-Area (GB/SA) model in AMBER 8 was chosen, which computes the polar component of the solvation free energy by the GB method and the non-polar component taken to be proportional to the solvent accessible surface area of the molecule with an experimentally obtained proportionality constant. The salt-concentration was set to a physiological value of 0.2 M. A large non-bonded cutoff of 25 Å for both electrostatics and Lennard-Jones interactions was used. Use of SHAKE [19] to constraint chemical bonds involving H-atoms allowed a time-step of 2-fs. After equilibrating *S1_pre* and *S2_pre* under the GB/SA model and using the Langevin thermostat to mimic solvent friction and stochastic effects at 300 K (using collision frequency of 1 ps^{-1}), the resultant structures (denoted *S1* and *S2*) served as starting points for our force-probe studies.

To carry out a force-probe MD simulation under constant-velocity, each group of atoms to be pulled (pull-group) has its center-of-mass restrained by a spring-like potential to some reference position. These positions or reference coordinates were then displaced successively by 1 Å along the pulling direction to apply a constant strain on the molecule. To *stretch* flagellin, the pulling direction "**CP**" lies along the line joining coordinate "**C**" in domain D3, being either the C_α atom of Gly211 ($\mathbf{C}_1$) or the C_α atom of Gly237 ($\mathbf{C}_2$), to coordinate "**P**" which denotes the center-of-mass of the termini C_α atoms (Fig. 2). The **CP** vector was initially oriented to the *x*-axis of the simulation system. To *Unzip* flagellin, the N- and C-terminal C_α atoms are displaced in opposite directions along a vector perpendicular to the *stretch* direction, either along *y*- or *z*-axis (see Table 1). The pulled atoms relax

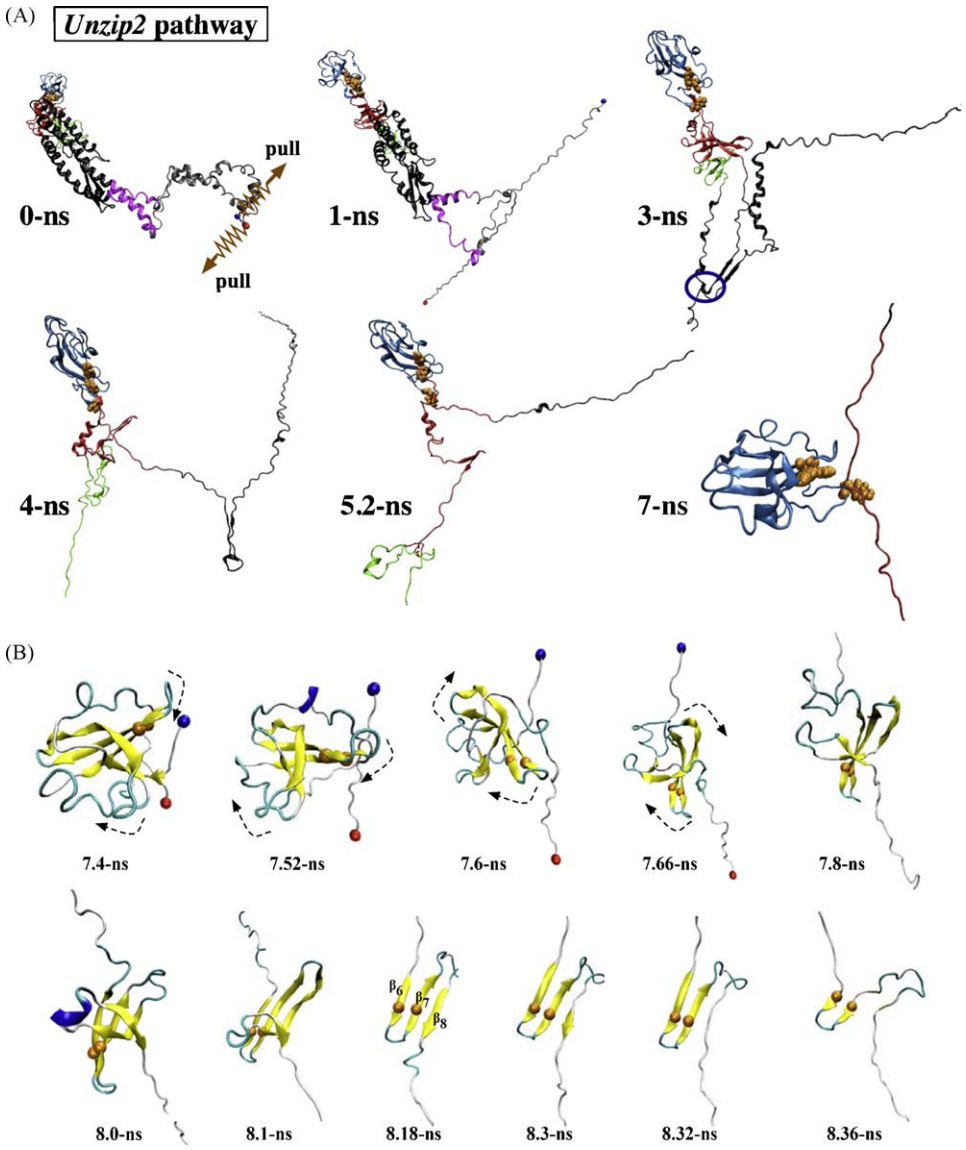

Fig. 2. Mechanical unfolding of flagellin under *Unzip*. (A) Trajectory snapshots from the *Unzip2* simulation illustrating the unraveling of domains D0, D1 and D2. Domains colored as in Fig. 1. Blue and red spheres represent the N- and C-terminal C_α atoms, denoted as A and B. Orange spheres represent atoms of the D3 surface three-residue aromatic cluster. Dark blue circle indicate the salt-bridge interaction between the D1 N-terminal hairpin and D1 C-terminal. (B) Detailed snapshots showing unraveling of domain D3. A rotation of the globular domain was observed and indicated by dashed arrows. N- and C-terminal alpha-carbon atoms of D3 are shown as blue and red spheres, respectively. Alpha-carbons of aromatic residues F222 and Y229 are shown as orange spheres.

Table 1
List of force-probe MD simulations conducted.

Sim.	Pulling direction[a]	v (Å/ps)[b]	Initial conf.[¶]	k[c]	Max ext. (Å)	Denat. time[a] (ns)	Denat. force[a] (pN)	Transport work[a] (kcal/mol)	Transport force[a] (pN)
Stretch1	$\mathbf{C_1P}$	0.05	*S1*	2	607	7.8	10,000	9730	3440
Stretch2	$\mathbf{C_1P}$	0.1	*S1*	2	822	4.1	12,270	7200	2500
Stretch3	$\mathbf{C_1P}$	0.25	*S1*	2	784	1.5	8000	10,230	2000
Stretch4	$\mathbf{C_1P}$	0.1	*S2*	2	716	4	11,550	–	–
Stretch5	$\mathbf{C_1P}$	0.1	*S1*	20	786	3.7	13,430	14,300	8000
Stretch6	$\mathbf{C_2P}$	0.1	*S1*	2	677	3.3	2630	7270	2100
Unzip1	*z*	0.05	*S1*	2	1614	16.9	1960	16,950	1960
Unzip2	*z*	0.1	*S1*	2	1652	8.3	1950	21,180	1950
Unzip3	*z*	0.25	*S1*	2	1738	3.3	3420	41,700	3420
Unzip4	*z*	0.1	*S2*	2	1590	8.6	1720	21,360	1720
Unzip5	*z*	0.1	*S1*	20	1600	8.5	2580	24,670	2580
Unzip6	*y*	0.1	*S1*	2	1770	8.2	1560	20,290	1560

For *Stretch4*, the D3 cross-section remained larger than 20 Å despite being denatured according to our criterion.
[a] See main text for the definition of directions.
[b] Pulling speed at each of the two ends.
[c] Probe/virtual spring constant k is given in units of kcal/mol Å^2.

towards the new positions in time intervals ranging from 4 to 20 ps, giving effective pulling speeds of 0.1–0.5 Å/ps. This *pseudo*-steered-MD approach offers two advantages: (i) no code modifications are needed and (ii) longer relaxation time interval (30–50 ps) could be used for a closer-to-equilibrium simulation in the spirit of the "pull-and-wait" scheme [20].

The deviation of the actual position $x(t)$ of the pull-group from the desired position $x_{REF}(t)$ (reference coordinates mentioned above) implies a harmonic restraint force $F(t) = k(x(t) - x_{REF}(t))$ exerted by the biomolecule on the virtual probe spring with force-constant k. This force is equal in magnitude but opposite in direction to the applied force. Our scheme approximates the conventional SMD approach when x_{REF} is incremented at smaller displacements over shorter relaxation intervals. Force-probe simulations conducted in this study are listed in Table 1. All force-probe simulations were performed with Sander module of AMBER 8 running on an in-house dual Xeon Linux cluster connected by a Gigabit-Ethernet network.

2.3. Analysis and visualization

The restraint forces were computed using TCL scripts executed under VMD [21]. The extension along the pulled direction in each simulation was obtained by projecting the instantaneous vector along the line connecting pulled-groups onto the pulling vector. The built-in Tachyon ray-tracer [22] in VMD was used for the rendering of molecular figures, with secondary structures assigned by STRIDE [23]. Residue contacts were computed using the Multiscale Modeling Tools for Structural Biology [24].

3. Results and discussion

Using force-probe MD, we have obtained the mechanical unfolding pathways of *Salmonella typhimurium* flagellin (a four-domain protein) when it is subjected to constant-velocity pulling along (*Stretch*) and perpendicular (*Unzip*) to its major principal axis. The two-end pulling simulations conducted in our study are listed in Table 1.

3.1. Detailed unfolding pathways

Trajectory snapshots from *Unzip2* (Fig. 2) and *Stretch2* (Fig. 3) simulations illustrate the respective unfolding pathways.

3.1.1. Unzipping flagellin

In all *Unzipping* simulations, the sequence of domain unfolding followed the arrangement of the domains from N- to C-terminal (Fig. 1): D_f1, D2b, D2a, D3. However, D3 was denatured before D2a if we initiate pulling only at the N-terminal (fixing the C-terminal) because D3 is N-terminal to D2a (data not shown). The salt-bridge across N-D1 Asp156 and C-D1 Arg431 (blue circle in Fig. 2A) has to be disrupted for the separation of the N-terminal half of D1 from the C-terminal half. After disruption of this native salt-bridge, non-native ones involving Arg431-Glu153 or Arg431-Asp151 delayed the separation of N-D1 and C-D1. However, no significant force peak was observed in the force–extension curves during D1 unfolding (see below) due to the relatively low mechanical resistance. In the denaturation of D2, the mostly β-stranded D2b lost its regular secondary structures under tension before being completely unraveled. This suggests that D2b may have low mechanical stability in addition to its low thermal stability suggested by us [5]. The unfolding of D3 seems to be hindered by a crisscrossing of its termini regions, which has to be resolved by a rotation (Fig. 2B upper row) upon tension built-up in the backbone before unraveling can continue. The transiently stable substructure in D3 is the β_{6-8} sheet, which unfolded via denaturation of β_8 (Fig. 2B lower row). The aromatic interaction between Phe222 and Tyr229 (C_α atoms shown as spheres in Fig. 3) could have enhanced the mechanical stability of $\beta_6\beta_7$ over that of $\beta_7\beta_8$, leading to preferential detachment of β_8 from the sheet.

3.1.2. Stretching flagellin

In the majority of our *Stretching* simulations, domain D_f1 (the proteolytic-resistant portion of D1, Fig. 1) denatured first as it is composed of α-helices which are less resistant to mechanical forces than the β-strand-rich domains D2 and D3, in agreement with theoretical work [25]. The unfolding of D2 requires the β-hairpin in D_f1 (green oval in Fig. 3) to be unfolded to allow for further extension of the backbones. Engineering a disulfide-bridge to stabilize the D_f1 hairpin against unfolding could stall the *Stretch* pathway but not affect the *Unzip* pathway. This might be one approach to probe the unfolding pathway experimentally. Sub-domain D2b either denatured before or in conjunction with D2a. D3 was usually the last domain to be completely denatured under *Stretch*, except under the fastest pulling rate or when we pull on Gly237 instead of Gly211 whereby D3 unfolded almost as quickly as D_f1. This is because Gly237 lies on the turn connecting β_7 to β_8

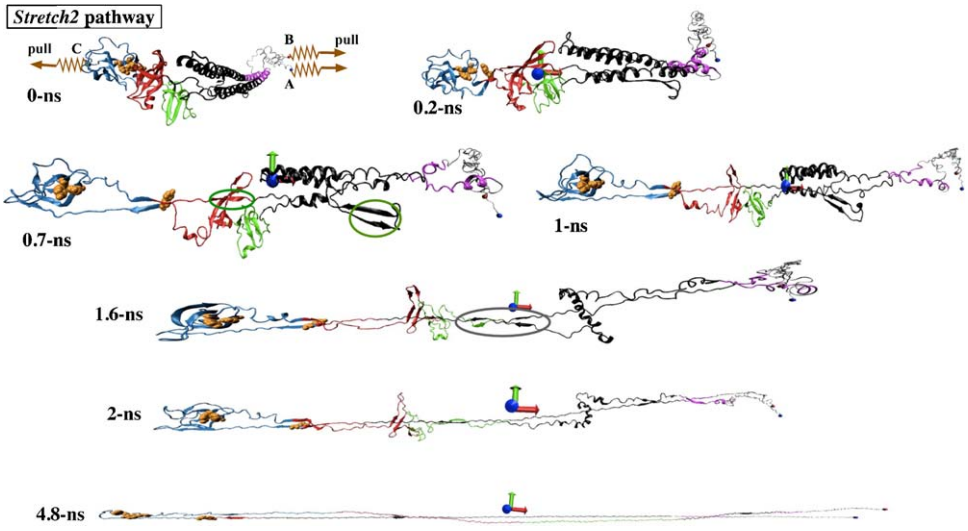

Fig. 3. Mechanical unfolding of flagellin under *Stretch*. Trajectory snapshots from the *Stretch2* simulation. Blue and red spheres represent the N- and C-terminal C_α atoms, denoted as A and B. Coordinate C is the C_α atom of G211. The pulling vector for *Stretch* is along the line connecting C to the center-of-mass of A and B. Coordinate axes mark the geometrical center of each snapshot. Colored ovals indicate load-bearing interactions (see text).

and hence pulling on Gly237 distorts the main $\beta_{6\text{-}8}$ "structural core" of D3 (Fig. 1). In contrast, Gly211 lies on a loop connecting helix α_4 and β_6, thus lying at the periphery of the "structural core". This suggests that mechanical resistance of D3 is dependent on pulling geometry, as found for many protein domains [11,12]. Lastly, we observed that the surface aromatic cluster (Tyr190-Phe222-Tyr229, orange spheres in Figs. 2 and 3) remained largely intact during *Unzip* until the unfolding of D3 but was disrupted early when flagellin domains are being aligned along the pulling direction during *Stretch*.

3.2. Force–extension profiles

The effect of changing the pulling speed, probe spring stiffness, initial conformation and pulling direction on the mechanical response are illustrated by force–extension curves in Fig. 4.

The force–extension curves for *Stretching* are shown in Fig. 4A–D. Changing the pulling speed do not significantly alter the force profile (Fig. 4A). The initial extension up to ~150 Å was produced by inter-domain movements and extension of domain linkers, with the protein aligning along the pulling vector without any domain unfolding. The curves overlap well and are almost linear with the slope representing the effective elastic spring constant of flagellin in this regime, estimated to be around 5 pN/Å. This so-called "tertiary structural elasticity" exhibited by modular extracellular matrix proteins under weak forces [28] was also insensitive to changes in the probe spring constant, the starting conformation or slight changes in the pulling vector (Fig. 4B–D). For extensions beyond 150 Å, use of a different initial conformation has little effect on the profile (Fig. 4B) but differences appear when we use a stiffer probe spring or change the pulling vector (Fig. 4C and D). A stiffer spring at the same pulling speed (giving a larger loading rate

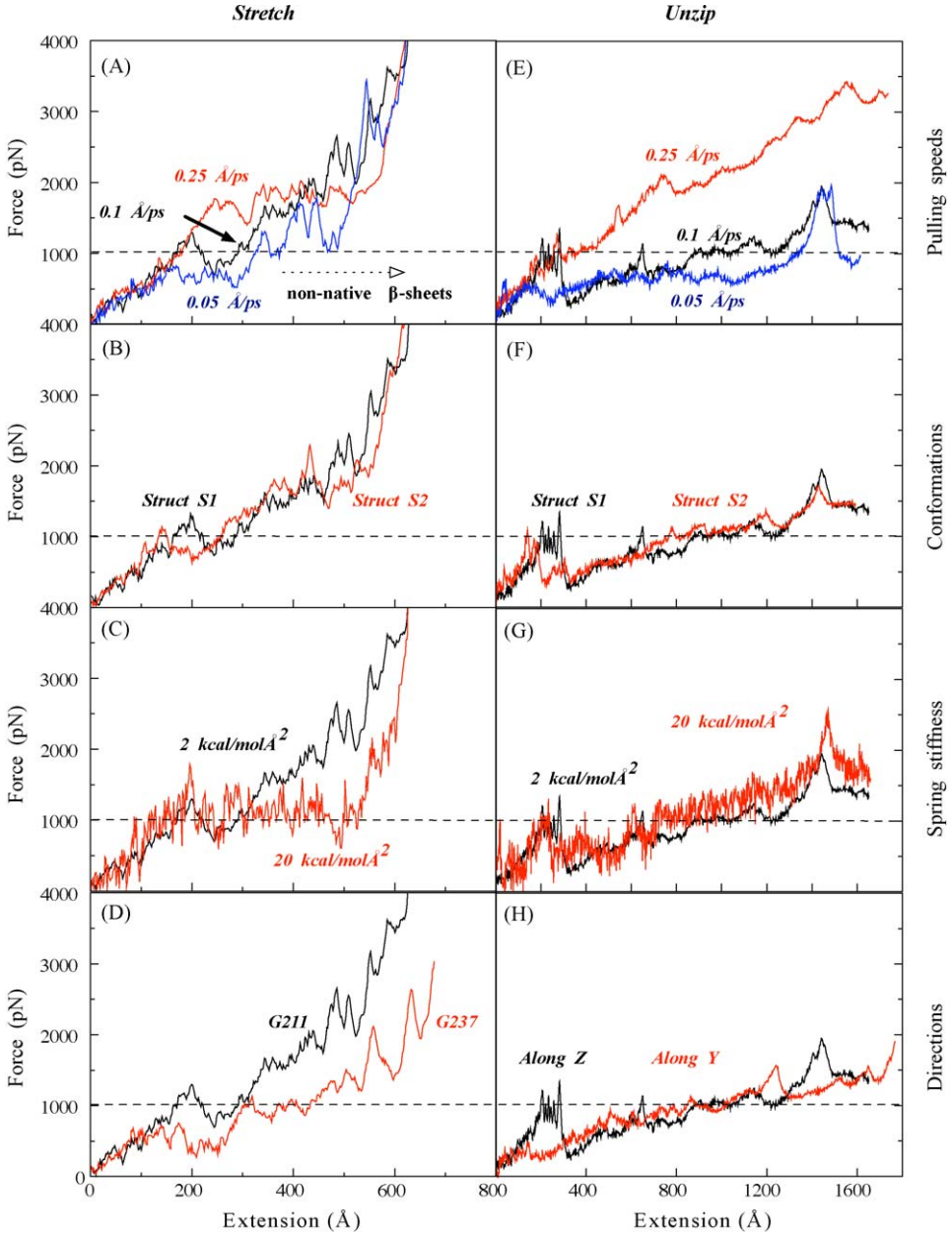

Fig. 4. Force–extension curves to show how various simulation conditions affect the mechanical response of flagellin from *Stretch* (left column) and *Unzip* (right column) simulations. Note the difference in the scale of the *x* axes. Data with forces above 4000 pN are omitted.

as the product of the effective spring constant of the system with the pulling speed) was more effective at overcoming the mechanical resistance of the molecule to unfold it rapidly. Changing the location in D3 at which the force is applied also has an effect on D3s mechanical stability. The domain denatured faster when Gly237 is pulled, leading to lower restraint forces measured. Formation of non-native anti-parallel β-sheets along the length of the unfolded backbone (gray oval in Fig. 2 and Fig. S1) that has to be disrupted for further extension and unfolding may have led to the continued increase in restraint forces after half of the maximum extension has been reached. D3 was found to maintain a cross-section of slightly over 20 Å (based on the C_α backbone) during the steep increase of force till around 550 Å. This observation suggests that a "thin enough" D3 could be difficult to produce even when the other domains have been highly denatured. The β-rich "structural core" takes significant effort to denature by elongation. Overall, flagellin appears rather stiff when pulled along its length.

The force–extension curves for *Unzipping* are shown in Fig. 4E–H. The use of larger probe spring stiffness or different starting conformations did not alter the force–extension profile significantly (Fig. 4F and G). However, the force–extension profiles were markedly different at different pulling speeds (Fig. 4E), with the effective stiffness (the slope of a linear fit to the curve) decreasing with slower pulling. At experimental pulling speeds, flagellin would be expected to appear even softer under *Unzip*. Forces remained below 1000 pN for the most part under the slowest speed investigated except at large extensions when D3 has to be unfolded. The sharp peak in restraint force at extension of 1400 Å for pulling speeds of 0.05 Å/ps and 0.1 Å/ps (Fig. 4E) is caused by the building up of tension in the polypeptide chain to enable the rotation of D3 to a more favorable orientation for its unraveling. On the other hand, a group of peaks at very low extension (at 0.1 Å/ps) was due to the formation of a non-native helical bundle in D0, which stalls unfolding. This backbone segment tangling is much less pronounced when we pull at the slower speed of 0.05 Å/ps. But if we rotate the pulling vector by 90°, we could avoid the helical bundling as well as the need to rotate D3 (see Fig. 4H). The only major force peak was then due to the separation of β_3 and β_{12} in D2a via lateral-shear (see below). Based on the above, we speculate that force–extension curve of flagellin unfolding under *Unzip* scheme in AFM might not contain any significant force peaks and would be rather featureless.

We have also attempted to get an estimate for the mechanical work required to produce a transport-capable flagellin conformation for each unfolding scheme. The "transport work" listed in Table 1 are computed from the areas under each force–extension curve from zero extension up till the extension at which flagellin becomes "thin enough" to fit into the channel. By "thin enough" we mean the largest cross-section of domain D3 (represented by its C_α backbone) is less than the channel diameter of 20 Å. However, we must point out that a more accurate comparison of the unfolding work under each scenario would involve discounting the dissipative work injected into the system during each of the non-equilibrium pulling simulations. The dissipative work can be computed based on the frictional drag experienced by the pulled atom [29]. But as the dissipative work for *Stretching* would intuitively be larger than for *Unzipping* because an atom in the globular domain D3 was pulled compared to N and C termini atoms, this would still result in a smaller reversible unfolding work for *Stretching* compared to *Unzipping*. Though *Stretching* might require less work than *Unzipping*, the corresponding "transport force" (defined as the maximum force encountered before flagellin becomes "thin enough") was larger for Stretching under the slower pulling speeds that we have used.

Furthermore, Lavery and co-workers found that the relative sliding of parallel or anti-parallel β-strands (β longitudinal-shear) takes twice the mechanical force of stretching α-helices and 10–25 times that of 'peeling apart' the same pair of β-strands from one end (β lateral-shear) [25]. This is because multiple backbone hydrogen bonds have to be broken simultaneously for longitudinal-shear whereas only individual ones need to be broken for lateral-shear. The much higher occurrence of longitudinal-shear over lateral-shear during *Stretch* simulations naturally resulted in much larger mechanical effort compared to *Unzip*. An absence in flagellin of disulphide-bridges, commonly used to strengthen extracellular protein domains, also suggests that flagellin needs to be completely unraveled (via *Unzip*) for efficient export.

3.3. Limitations of our study

In order to observe denaturation on the nanosecond time-scale, the pulling speeds we have used in our *in silico* mechanical unfolding of flagellin are at least a million times larger than those employed in force-spectroscopy experiments like AFM. This resulted in peak unfolding forces that are typically 4–10 times larger than in experiment [15] (also inferred from the Biomolecule Stretching Database: www.ifpan.edu.pl/BSDB).

We have employed implicit solvent model out of need, despite that its use in simulated mechanical unfolding remains controversial. On one hand, the replacement of backbone hydrogen bonds by those made to solvent molecules have been found to be important in the unfolding process probed by explicit solvent force-probe/SMD simulations [20,26]. A force-spectroscopy study confirmed that solvent molecules are an integral part of the unfolding transition state [27]. On the other hand, the use of implicit solvent avoided the slow discrete solvent response under the high pulling rates used in most force-probe/SMD simulations, pointed out by Paci and Karplus [28].

Our work only investigated two intuitive but extreme unfolding pathways for flagellin to become sufficiently unfolded for transport through the filament channel. In reality other unfolding scenarios may be envisioned, such as one-termini pulling or pull-relax cycles (where unfolded segments are not pulled upon but just migrate into the channel via diffusion) that may incur a lower mechanical effort than the constant pulling scenarios we have considered here.

4. Conclusions

During bacterial flagellar filament assembly, the subunit protein flagellin has to be exported from within the cytoplasm to the tip of the growing filament via a narrow 20 Å channel. It is likely that flagellin has to undergo unfolding to become transport-capable. In this work, we have used force-probe molecular dynamics simulations to mechanically unfold flagellin under two schemes. In one scheme, the "folded-back" flagellin is unraveled from its termini in an unzipping fashion to eventually result in a linear polypeptide. In the other scheme, flagellin is elongated along its length while preserving the arrangement of its four domains. We have obtained atomic-level unfolding pathways and quantified the mechanical efforts required under each scheme. We found that unraveling the multi-domain protein from its adjacently placed termini was zipper-like and encountered lower unfolding forces with only lateral-shearing of β-sheets where single H-bonds are broken at a time.

Our work lead to some interesting speculations: do HVR domains in flagellin homologues also contain high proportion of β-sheets that are arranged to be easily unraveled via β lateral-shear, in spite of the lack of sequence conservation? These β-sheets might

also help to nucleate the re-folding process as suggested by our thermal unfolding study [10]. Do such design principles extend to other β-rich proteins that are exported in the flagellar or other type-III secretion systems? An understanding of how proteins may be designed for structural stability and ease of mechanical denaturation for transport may find application in bio-nanotechnology.

Acknowledgements

This work was supported by the Next Generation Super Computing Project, Nanoscience Program, Grant-in-Aid for Scientific Research (B) and Grants-in-Aid for Scientific Research on Priority Areas from the Ministry of Education, Culture, Sports, Science and Technology (MEXT) of Japan to A.K. C.-P.C. gratefully acknowledges the support of a MEXT graduate scholarship. The authors would also like to thank the anonymous reviewer for her/his valuable comments.

Appendix A. Supplementary data

Supplementary data associated with this article can be found, in the online version, at doi:10.1016/j.jmgm.2009.11.007.

References

[1] R.M. Macnab, How bacteria assemble flagella, Annu. Rev. Microbiol. 57 (2003) 77–100.
[2] T. Ikeda, S. Yamaguchi, H. Hotani, Flagellar growth in a filament-less Salmonella fliD mutant supplemented with purified hook-associated protein 2, J. Biochem. (Tokyo) 114 (1993) 39–44.
[3] K. Yonekura, S. Maki-Yonekura, K. Namba, Complete atomic model of the bacterial flagellar filament by electron cryomicroscopy, Nature 424 (2003) 643–650.
[4] S.A. Beatson, T. Minamino, M.J. Pallen, Variation in bacterial flagellins: from sequence to structure, Trends Microbiol. 14 (2006) 151–155.
[5] A. Kitao, K. Yonekura, S. Maki-Yonekura, F.A. Samatey, K. Imada, K. Namba, N. Go, Switch interactions control energy frustration and multiple flagellar filament structures, Proc. Natl. Acad. Sci. U.S.A. 103 (2006) 4894–4899.
[6] A.J. Ozin, L. Claret, F. Auvray, C. Hughes, The FliS chaperone selectively binds the disordered flagellin C-terminal D0 domain central to polymerisation, FEMS Microbiol. Lett. 219 (2003) 219–224.
[7] A. Muskotal, R. Kiraly, A. Sebestyen, Z. Gugolya, B.M. Vegh, F. Vonderviszt, Interaction of FliS flagellar chaperone with flagellin, FEBS Lett. 580 (2006) 3916–3920.
[8] S. Prakash, A. Matouschek, Protein unfolding in the cell, Trends Biochem. Sci. 29 (2004) 593–600.
[9] J.E. Galán, Energizing type III secretion machines: what is the fuel? Nat. Struct. Mol. Biol. 15 (2008) 127–128.
[10] C.-P. Chng, A. Kitao, Thermal unfolding simulations of bacterial flagellin: insight into its refolding before assembly, Biophys. J. 94 (2008) 3858–3871.
[11] M. Carrion-Vazquez, H. Li, H. Lu, P.E. Marszalek, A.F. Oberhauser, J.M. Fernandez, The mechanical stability of ubiquitin is linkage dependent, Nat. Struct. Biol. 10 (2003) 738–743.
[12] H. Dietz, F. Berkemeier, M. Bertz, M. Rief, Anisotropic deformation response of single protein molecules, Proc. Natl. Acad. Sci. U.S.A. 103 (2006) 12724–12728.
[13] T. Sato, M. Esaki, J.M. Fernandez, T. Endo, Comparison of the protein-unfolding pathways between mitochondrial protein import and atomic-force microscopy measurements, Proc. Natl. Acad. Sci. U.S.A. 102 (2005) 17999–18004.
[14] H. Grubmüller, B. Heymann, P. Tavan, Ligand binding: molecular mechanics calculation of the streptavidin–biotin rupture force, Science 271 (1996) 997–999.
[15] H. Lu, B. Isralewitz, A. Krammer, V. Vogel, K. Schulten, Unfolding of titin immunoglobulin domains by steered molecular dynamics simulation, Biophys. J. 75 (1998) 662–671.
[16] S. Ohta, M.T. Alam, H. Arakawa, A. Ikai, Origin of mechanical strength of bovine carbonic anhydrase studied by molecular dynamics simulation, Biophys. J. 87 (2004) 4007–4020.
[17] S.P. Ng, R.W. Rounsevell, A. Steward, C.D. Geierhaas, P.M. Williams, E. Paci, J. Clarke, Mechanical unfolding of TNfn3: the unfolding pathway of a fnIII domain probed by protein engineering, AFM and MD simulation, J. Mol. Biol. 350 (2005) 776–789.
[18] A. Onufriev, D. Bashford, D.A. Case, Exploring protein native states and large-scale conformational changes with a modified generalized born model, Proteins 55 (2004) 383–394.
[19] J.-P. Ryckaert, G. Ciccotti, H.J. Berendsen, Numerical integration of the Cartesian equations of motion of a system with constraints: molecular dynamics of n-alkanes, J. Comput. Phys. 23 (1977) 327–341.
[20] G. Pabón, L.M. Amzel, Mechanism of titin unfolding by force: insight from quasi-equilibrium molecular dynamics calculations, Biophys. J. 91 (2006) 467–472.
[21] W. Humphrey, A. Dalke, K. Schulten, VMD: visual molecular dynamics, J. Mol. Graph. 14 (1996) 33–38.
[22] J. Stone, An efficient library for parallel ray tracing and animation, Masters thesis, Computer Science Department, University of Missouri-Rolla, 1998.
[23] D. Frishman, P. Argos, Knowledge-based protein secondary structure assignment, Proteins 23 (1995) 566–579.
[24] M. Feig, J. Karanicolas, C.L. Brooks, MMTSB Tool Set: enhanced sampling and multiscale modeling methods for applications in structural biology, J. Mol. Graph. Model. 22 (2004) 377–395.
[25] R. Rohs, C. Etchebest, R. Lavery, Unraveling proteins: a molecular mechanics study, Biophys. J. 76 (1999) 2760–2768.
[26] M. Gao, M. Sotomayor, E. Villa, E.H. Lee, K. Schulten, Molecular mechanisms of cellular mechanics, Phys. Chem. Chem. Phys. 8 (2006) 3692–3706.
[27] L. Dougan, G. Feng, H. Lu, J.M. Fernandez, Solvent molecules bridge the mechanical unfolding transition state of a protein, Proc. Natl. Acad. Sci. U.S.A. 105 (2008) 3185–3190.
[28] E. Paci, M. Karplus, Unfolding proteins by external forces and temperature: the importance of topology and energetics, Proc. Natl. Acad. Sci. U.S.A. 97 (2000) 6521–6526.
[29] M. Balsera, S. Stepaniants, S. Izrailev, Y. Oono, K. Schulten, Reconstructing potential energy functions from simulated force-induced unbinding processes, Biophys. J. 73 (1997) 1281–1287.